RAPID COMMUNICATIONS

PHYSICAL REVIEW B VOLUME 44, NUMBER 19 15 NOVEMBER 1991-I

Reconstruction at ordered Au(110)-aqueous interfaces as probed by atomic-resolution scanning tunneling microscopy

Xiaoping Gao, Antoinette Hamelin,* and Michael J. Weaver
Department of Chemistry, Purdue University, West Lafayette, Indiana 47907
(Received 15 May 1991; revised manuscript received 19 August 1991)

Atomic-resolution scanning-tunneling-microscopy images of ordered Au(110) in aqueous 0.1*M* $HClO_4$, reported as a function of electrode potential, provide an unusually detailed picture of surface reconstruction. Lowering the potential of a freshly annealed surface to −0.3 V versus saturated calomel electrode (SCE) yield images consisting primarily of domains having (1×2) symmetry. While the (1×2) structure exhibits an atomic density commensurate with the usual "missing-row" model, the images suggest that significant relaxation of both top- and second-layer atoms occurs. Three-atom-wide ribbons, lying along the [1$\bar{1}$0] direction, are seen to provide the basic building blocks of the reconstruction; these units also yield "added-row" domains of (1×*n*) symmetry, with *n*=3 or higher. The reconstruction is lifted, yielding the (1×1) Au(110) surface, rapidly (within ~2 s) upon altering the potential to 0 V vs SCE, yet reappears immediately upon returning to −0.3 V.

As for metal surfaces in ultrahigh vacuum (UHV), elucidating the occurrence and nature of reconstruction at ordered electrochemical interfaces is a topic of major fundamental and practical importance. While reconstruction has long been considered to occur at metal-solution interfaces, especially for gold low-index faces on the basis of conventional electrochemical measurements,[1] detailed information has been lacking due to the paucity of suitable *in situ* structural probes. Both second-harmonic generation[2] (SHG) and x-ray diffraction[3] have recently proved useful as *in situ* probes at ordered gold electrodes. However, the former yields little structural information, and the latter approach is limited in part by the availability of synchrotron x-ray sources.

A very promising technique for this purpose is scanning tunneling microscopy (STM) since it can yield local real-space structural information. While few STM studies of *in situ* electrochemical systems have achieved the necessary atomic resolution, some recent reports demonstrate that such STM images can be observed under favorable circumstances at metal-solution interfaces.[4–8] One such study from our laboratory, involving Au(100) in aqueous 0.1*M* $HClO_4$, illustrates that remarkably detailed information on potential-induced surface reconstruction can be obtained from *in situ* STM.[8] Specifically, the (1×1) Au(100) surface is transformed into corrugated quasihexagonal domains having primarily a (5×27) symmetry by altering the potential below −0.25 V versus saturated calomel electrode (SCE); the reconstruction can be lifted by returning to 0.2 V.

Reported here is a preliminary account of related measurements performed for Au(110). The reconstruction of this surface in UHV has been examined extensively by low-energy electron diffraction (LEED),[9–11] ion scattering,[12–14] x-ray diffraction,[15] electron microscopy,[16] and STM.[17] A predominantly (1×2) symmetry is observed, which is most commonly interpreted in terms of a "missing- (or added-) row" structure [e.g., Ref. 15(b)]. Besides giving uniquely detailed information of such reconstruction on the Au(110) electrochemical surface, the present STM images provide some insight into the formation mechanism.

The Au(110) crystal (hemisphere, 5 mm diameter) was grown, cut, and polished in LEI-CNRS as outlined in Ref. 18. The crystal was flame annealed immediately before each experiment, cooled in ultrapure water, and transferred to the STM cell protected by a drop of water. Details of the *in situ* STM procedures are mostly as outlined in Refs. 8 and 19. The microscope is a commercial Nanoscope II instrument (Digital Instruments, Inc.). The atomic-resolution STM images were obtained in the constant-current mode. The set-point current i_t was typically 20–30 nA, and the bias voltage V_b was usually 4–10 mV. After assembling the STM cell with the freshly annealed crystal, aqueous 0.1*M* $HClO_4$ was added, and a cyclic voltammogram (50 $mV s^{-1}$) usually recorded to check the surface state.

Unlike Au(100),[8] satisfactory atomic-resolution images were usually not obtained initially at potentials within the range −0.1 to 0.2 V vs SCE. However, altering the potential to −0.3 to −0.4 V yielded atomic-resolution images of consistently high quality. Figure 1 shows a typical *unfiltered* large-scale (180×180 $Å^2$) image obtained at −0.3 V vs SCE. (The height-shaded view is 30° from the surface normal.) Stacked sets of parallel ribbon segments, located along the [1$\bar{1}$0] direction, are clearly seen. The spacing between these ribbons is mostly 4.0*n* Å, where *n*=2 or 3, i.e., corresponding to (1×2) and (1×3) symmetries. Figure 2 is a top view atomic-resolution image of a smaller (90×90 $Å^2$) region. Each ribbon is clearly seen to consist of three parallel rows of gold atoms. The interatomic spacing along the [1$\bar{1}$0] direction is 2.9±0.2 Å, i.e., as for unreconstructed Au(110).

A closeup of a region containing mostly (1×2) reconstruction is shown in Fig. 3. Information on the detailed surface atomic structure can be obtained from such STM images. While the overall symmetry and atomic density is consistent with the commonly proposed missing-row model, the present images indicate that some surface relaxation occurs, involving both the top and underlying atoms.

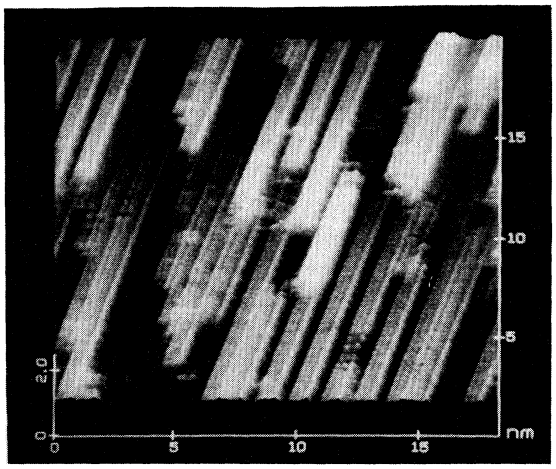

FIG. 1. Unfiltered large-scale STM image, shown as height-shaded plot 30° from surface normal, of reconstruction on ordered Au(110) in 0.1M $HClO_4$ at -0.3 V vs SCE.

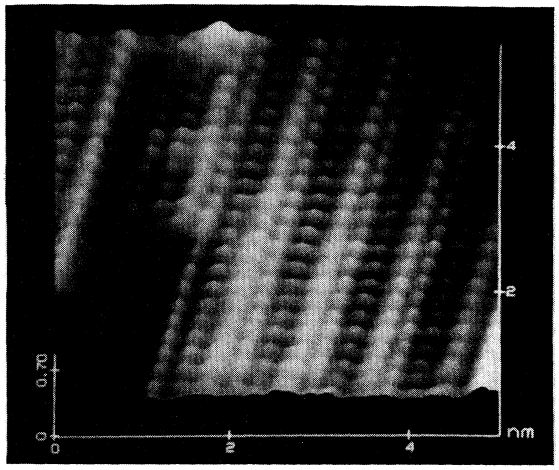

FIG. 3. Height-shaded close-up image of largely (1×2) domain.

In the conventional missing-row structure [depicted in Fig. 4(a)] the pairs of (unshaded) atoms either side of the central [1$\bar{1}$0] furrows are equivalent. The STM images, however, show that one of these rows in each unit cell is shifted by 1.45 Å along the [1$\bar{1}$0] direction, the atoms of which appear less intense (i.e., are depressed in the Z direction). Both these observations suggest that relaxation occurs so to form a slightly asymmetric structure as depicted in Fig. 4(b). This ball model shows that such a top-layer relaxation should be accompanied by some pairing of the second-layer atoms, as can be seen in the side view of Fig. 4(b). Also consistent with this relaxed structure are the corrugations obtained from the *constant-current* STM images, which indicate that the Z displacements of the b and c atoms [see Fig. 4(b)] are 0.2–0.3 Å and 0.4–0.6 Å, respectively, below atom a. These observed Z corrugations are markedly smaller than those anticipated for the unrelaxed missing-row structure [Fig. 4(a)].

A height-shaded STM image of a (1×3) surface region is shown in Fig. 5. (Note that the crystal has been rotated counterclockwise by ~40° compared with the earlier figures.) Unlike the (1×2) structure, the rows of atoms on either side of the highest (i.e., brightest) rows are virtually unshifted along the [1$\bar{1}$0] direction. In this respect, then, the (1×3) structure seen here is similar to the usual double missing-row model.

Altering the potential in the positive direction resulted in an immediate (within 2 s) disappearance of the reconstructed surface images by 0 V vs SCE, being replaced by images indicative of a (1×1) surface. Such an image is shown in Fig. 6. The (1×1) nature of the surface is evident from the spacing (4 ± 0.2 Å) between the rows along the [001] direction. These potential-induced structural changes are largely reversible as well as rapid, the recon-

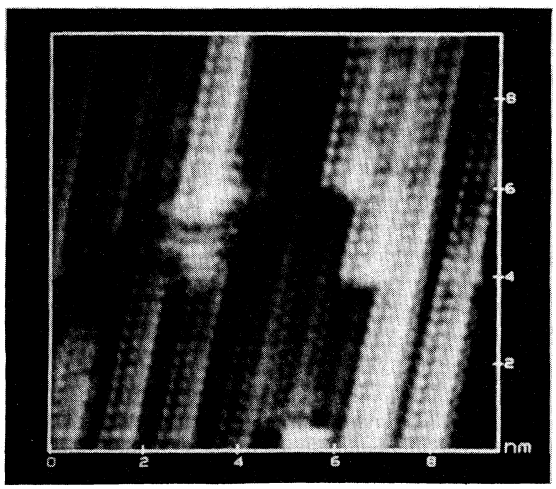

FIG. 2. Top view image showing (1×2) and (1×3) regions.

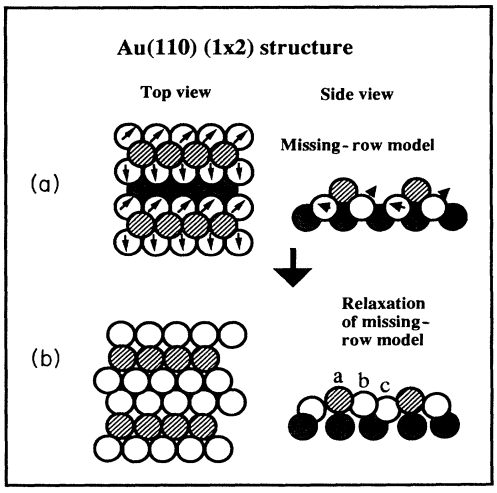

FIG. 4. Ball-model (1×2) structures for (a) conventional missing-row model and (b) with relaxation as suggested by the STM images.

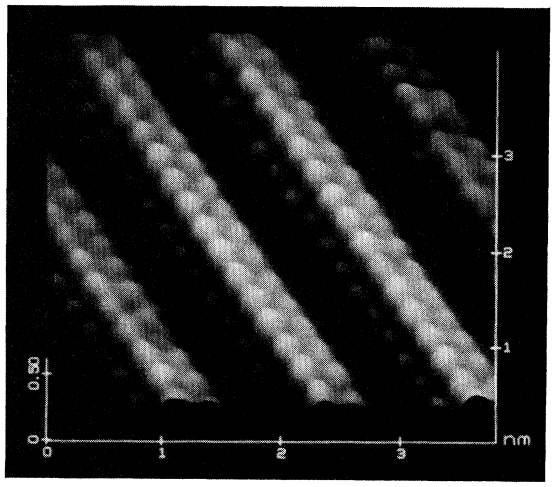

FIG. 5. Height-shaded image of (1×3) domain.

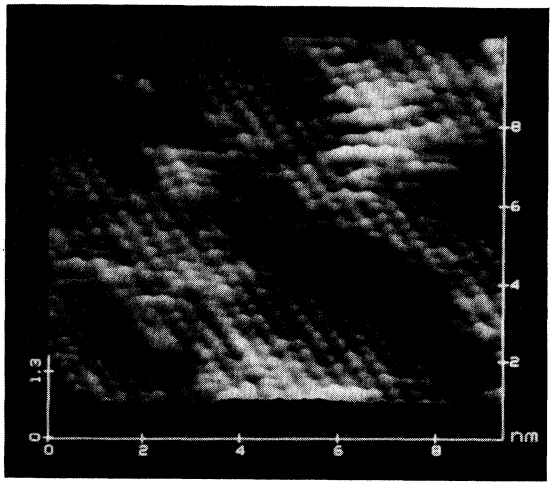

FIG. 6. Height-shaded image of (1×1) domain, formed by altering potential to 0 V vs SCE.

struction reappearing within ~2 s when the potential is returned to −0.3 V.

Further inspection of the STM images provides some insight into the mechanism of reconstruction. The three-atom-wide ribbons appear to provide basic building blocks from which the reconstruction is propagated. Examination of Fig. 1 shows that the longer-scale [i.e., (1×3), (1×4)] reconstructions occur by depositing such ribbons along the $[1\bar{1}0]$ direction on the underlying terrace. In this sense, therefore, these structures can be viewed as "added-", rather than "missing-", row domains. The concerted motion of atoms required to form (or remove) such reconstructions appear to involve migration both across and along the rows. The small and rather irregular domain sizes observed here on Au(110) (e.g., Fig. 1) suggest that only short-range atomic motion is required.

The present results bear a similarity to *in situ* STM data obtained on Au(100) in 0.1*M* $HClO_4$, described elsewhere,[8] in that extensive reconstruction appears on both surfaces at ~ −0.3 V and is lifted at 0 and 0.2 V vs SCE for Au(110) and (100), respectively. An important difference, however, is that these structural transformations are much more rapid (as well as more reversible) on Au(110), requiring ~10 min on Au(100). The latter slow kinetics are consistent with the 24% additional gold atoms needed to form the reconstructed Au(100) surface,[8] presumably provided by long-range diffusional transport. The more rapid reconstruction dynamics on Au(110) are consistent with the requirement of only short-range motion of the ribbon segments.

It is worth noting that the reconstruction on Au(110), as for Au(100), proceeds at potentials somewhat below the potential of zero charge [−0.02 V vs SCE for Au(110) in perchlorate media[20]], i.e., at small negative values of the surface electronic charge density, σ^m. While (1×2) reconstruction of clean Au(110) in UHV (i.e., at $\sigma^m=0$) is spontaneous at room temperature, the formation of (1×3) as well as (1×5) structures is observed upon the deposition of alkali metals.[21] Since adsorption of such ionizable metals will yield negative σ^m values, some correspondence to the electrochemical case might be anticipated. Interestingly, adjusting σ^m to negative values is predicted to encourage reconstruction on (110) surfaces as a result of minimizing the kinetic energy of the *sp* electrons.[22]

The observation of (1×2) and (1×3) reconstruction on clean Au(110) at negative potentials in perchloric acid is in qualitative accord with LEED measurements following electrode emersion.[11] Inconsistent with the present results, however, is the report in Ref. 11 that lifting the reconstruction on Au(110) requires large positive potentials, above 0.9 V vs SCE, where anodic oxide is formed. Given the facile nature of the Au(110) reconstruction process observed here, a rationalization of this discrepancy is that surface reconstruction on Au(110) is regenerated upon electrode emersion under the conditions in Ref. 11 except in the presence of surface oxide. The results here may, therefore, signal a significant limitation of the use of electrode emersion, as opposed to strictly *in situ* measurements (as for STM), as a means of probing surface reconstruction at electrochemical surfaces.

Dr. Si-Chung Chang provided valuable assistance in the gold crystal preparation. This work is supported by the National Science Foundation and the Office of Naval Research.

*Permanent address: Laboratorie d'Electrochimie Interfaciale du CNRS, 1 Place A. Briand, 92195 Meudon, France.

[1]A. Hamelin, J. Electroanal. Chem. **142**, 299 (1982).

[2]A. Friedrich, B. Pettinger, D. M. Kolb, G. Lüpke, R. Steinhoff, and G. Marowsky, Chem. Phys. Lett. **163**, 123 (1989).

[3]B. M. Ocko, J. Wang, A. Davenport, and H. Isaacs, Phys. Rev. Lett. **65**, 1466 (1990).

[4]O. M. Magnussen, J. Hotlos, R. J. Nichols, D. M. Kolb, and R. J. Behm, Phys. Rev. Lett. **64**, 2929 (1990).

[5]S.-C. Yau, C. M. Vitus, and B. C. Schardt, J. Am. Chem. Soc. **112**, 3677 (1990).

[6]S.-L. Yau, X. Gao, S.-C. Chang, B. C. Schardt, and M. J. Weaver, J. Am. Chem. Soc. **113**, 6049 (1991).

[7]C. M. Vitus, S.-C. Chang, B. C. Schardt, and M. J. Weaver, J. Phys. Chem. **95**, 7559 (1991).

[8]X. Gao, A. Hamelin, and M. J. Weaver, Phys. Rev. Lett. **67**, 618 (1991); and (unpublished).

[9]D. Wolf, H. Jagodzinski, and W. Moritz, Surf. Sci. **77**, 265 (1978); W. Moritz and D. Wolf, Surf. Sci. **163**, L655 (1985).

[10]J. R. Noonan and H. L. Davis, J. Vac. Sci. Technol. **16**, 587 (1979).

[11]M. S. Zei, G. Lehmpful, and D. M. Kolb, Surf. Sci. **221**, 23 (1989); R. Michaelis and D. M. Kolb, Surf. Sci. **234**, 6281 (1990).

[12]S. H. Overbury, W. Heiland, D. M. Zehner, S. Datz, and R. S. Thoe, Surf. Sci. **109**, 239 (1981).

[13]M. Copel and T. Gustafson, Phys. Rev. Lett. **57**, 723 (1986).

[14]J. Möller, H. Niehus, and W. Heiland, Surf. Sci. **166**, L111 (1986).

[15](a) I. K. Robinson, Phys. Rev. Lett. **50**, 1145 (1983); (b) E. Vlieg, I. K. Robinson, and K. Kern, Surf. Sci. **233**, 248 (1990).

[16]L. D. Marks, Phys. Rev. Lett. **51**, 1000 (1983).

[17]G. Binnig, H. Rohrer, Ch. Gerber, and E. Weibel, Surf. Sci. **131**, L379 (1983); T. Gritsch, D. Coulman, R. J. Behm, and G. Ertl, Surf. Sci. (to be published).

[18]A. Hamelin, S. Morin, J. Richer, and J. Lipkowski, J. Electroanal. Chem. **285**, 249 (1990).

[19]S.-C. Chang, S.-L. Yau, B. C. Schardt, and M. J. Weaver, J. Phys. Chem. **95**, 4787 (1991).

[20]A. Hamelin and M. J. Weaver, J. Electroanal. Chem. **223**, 171 (1987).

[21]P. Häberle, P. Fenter, and T. Gustafsson, Phys. Rev. B **39**, 5810 (1989).

[22]K-M. Ho and K. P. Bohnen, Phys. Rev. Lett. **59**, 1833 (1987).

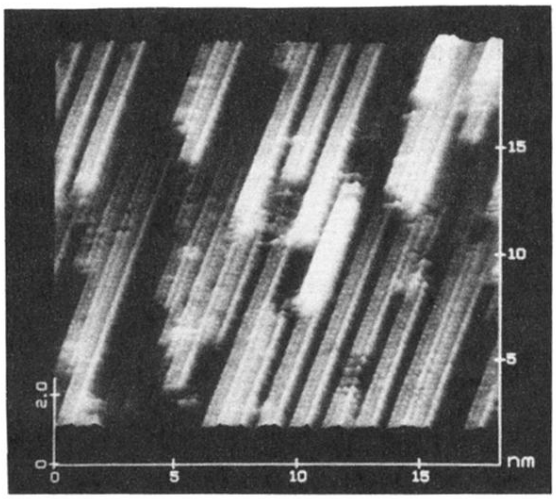

FIG. 1. Unfiltered large-scale STM image, shown as height-shaded plot 30° from surface normal, of reconstruction on ordered Au(110) in 0.1*M* $HClO_4$ at −0.3 V vs SCE.

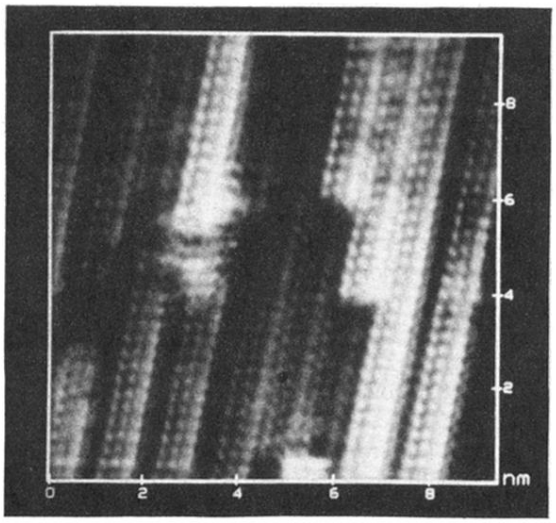

FIG. 2. Top view image showing (1×2) and (1×3) regions.

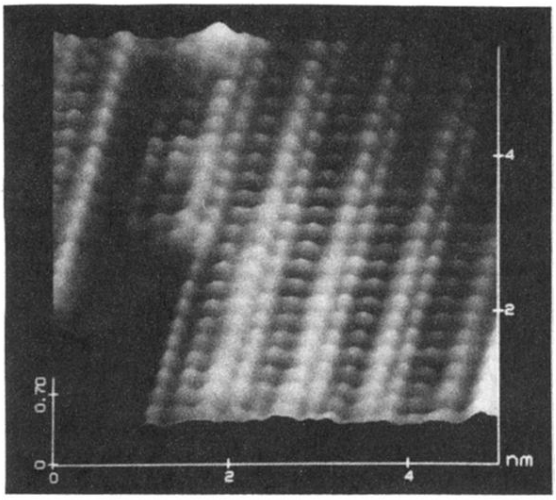

FIG. 3. Height-shaded close-up image of largely (1×2) domain.

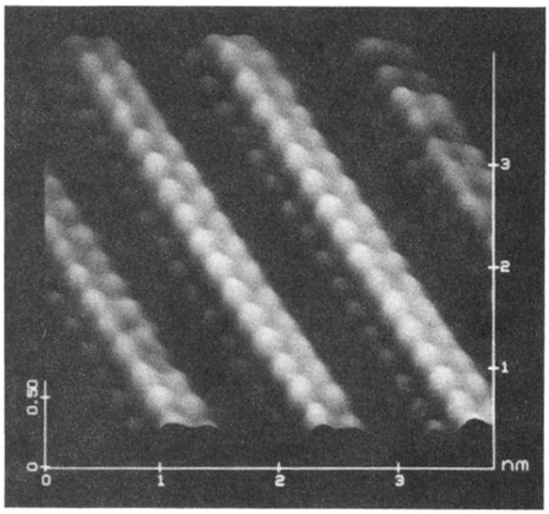

FIG. 5. Height-shaded image of (1×3) domain.

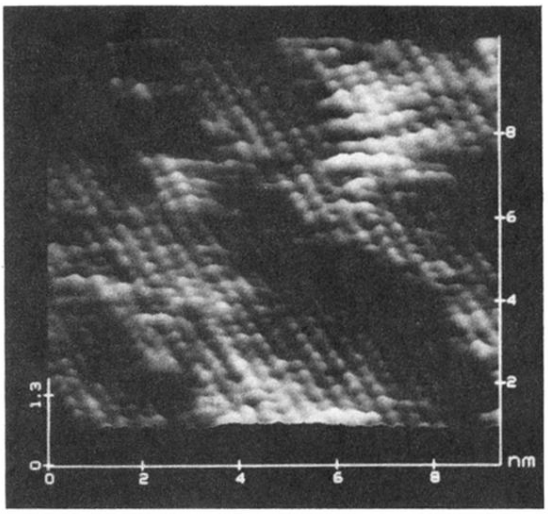

FIG. 6. Height-shaded image of (1×1) domain, formed by altering potential to 0 V vs SCE.